

The decoloration and mineralization of azo dye C.I. Acid Red 14 by sonochemical process: Rate improvement via Fenton's reactions

Jun-jie Lin^{a,b}, Xiao-song Zhao^b, Dan Liu^c, Zhi-guo Yu^{a,b}, Ying Zhang^a, Hui Xu^{a,*}

^a Key Laboratory of Terrestrial Ecological Process, Institute of Applied Ecology, Chinese Academy of Sciences, Shenyang 110016, China

^b College of Resources and Environment, Jinlin agricultural University, Changchun 130000, China

^c Agricultural college of Yanbian University, Yanji 130000, China

Received 14 November 2007; received in revised form 6 January 2008; accepted 7 January 2008

Available online 20 January 2008

Abstract

The degradation of azo dye C.I. Acid Red 14 (AR14) was investigated using cast iron in the absence and presence of low frequency ultrasound (59 kHz). The effects of pH, amount of cast iron ($[Fe]_0$) and initial concentration of AR14 ($[dye]_0$) on the degradation of AR14 by cast iron combined with low frequency ultrasound had been assessed. The degradation followed the first-order kinetics model. The first-order rate constant of AR14 degradation by cast iron was $7.50 \times 10^{-2} \text{ min}^{-1}$ while that by US-cast iron was $2.58 \times 10^{-1} \text{ min}^{-1}$. A 3.4-fold increase in the reaction rate was observed in the presence of ultrasound compared with that of absence of ultrasound. This kinetic effect is quantitatively accounted for a simple kinetic model based on the reaction of Fe(II) from cast iron in aqueous solution with sonochemically produced H_2O_2 (Fenton's reaction). This latter effect illustrates a simple way of achieving a substantial improvement in the efficiency of sonochemical degradation reactions. It was found that for azo dye AR14, the rate of color decay was the first order with respect to the visible absorption of the dye. The destruction of the naphthalene rings in azo dyes was slower than that of color. A significant mineralization of AR14 was observed.

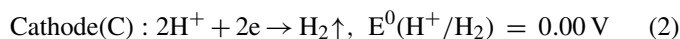
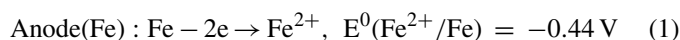
© 2008 Elsevier B.V. All rights reserved.

Keywords: Azo dye; Low frequency; Fenton's reaction; Cast iron; Mineralization

1. Introduction

Textile industries have shown a significant increase in the use of synthetic complex organic dyes as the coloring material [1]. The annual world production of textiles is about 30 million tones requiring 0.7 million tones of different dyes per year [2]. Degradation of dyes especially azo dyes, which contribute to about 70% of all used dyes, is difficult due to their complex structure and synthetic nature [3]. Azo dyes are characterized by nitrogen to nitrogen double bond ($-N=N-$). The color of dyes is due to azo bond and associated chromophores [4,5]. Strong color imparted by the dyes poses aesthetic problem and serious ecological problems such as inhibition of benthic photosynthesis and carcinogenicity [6,7]. Due to their biological recalcitrance, conventional biological treatment processes such as activated sludge process are ineffective to remove these dyes from wastewater [8,9].

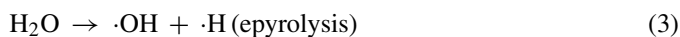
It is well known that the cast iron is an alloy and the main element is Fe and C. When the cast iron immerses in dye wastewater, many batteries are formed due to potential difference of electrode between Fe and C which has been one of the most effective pretreatment methods of the wastewater [10,11]. Fe is anode and C is cathode. In the acid case, the electrochemical reaction is as follows [12]:



[H] is able to break the chain of some organic compounds and change organic functional group, while Fe^{2+} is a good coagulant, it can adsorb reactant and achieve the aim of removal of pollutants. In the presence of ultrasonic cavitation, the efficiency of the degradation can be enhanced [13–17]. The power of ultrasonic cavitation to induce oxidation/destruction reactions is based on cavitation phenomenon, which consists of the formation, growth and collapse of acoustic bubbles [18]. When a liquid is sonicated, molecules of dissolved gases are entrapped

* Corresponding author. Tel.: +86 24 83970369; fax: +86 24 83970300.
E-mail address: xuhui@iae.ac.cn (H. Xu).

by microbubbles, which grow and expand at rarefaction of the acoustic cycle and release extreme temperatures upon adiabatic collapse [19,20]. Under such conditions, gas molecules inside the bubbles are pyrolytically fragmented into radical species, some of which diffuse into the aqueous phase to promote oxidation of organic matter. A simple scheme showing radical formation and depletion during water sonolysis is given below [19,21]:



So, a simple kinetic model based on the reaction of Fe(II) with sonochemically produced H_2O_2 (Fenton's reaction) can be seen from Eqs. (1) and (6). In this study, this latter effect on the degradation of a classical azo dye viz. C.I. Acid Red 14 (AR14) by cast iron in the absence and presence of ultrasound was investigated. Effects of initial pH values, amount of cast iron ($[\text{Fe}]_0$) and initial concentration of AR14 ($[\text{dye}]_0$) were studied in the process of US–cast iron in detail. In addition, AR14 and its degradation products were also analyzed by a UV–vis spectrophotometer and liquid chromatography–mass spectrometry (LC–MS).

2. Materials and methods

2.1. Reagents

AR14 was obtained from Shenyang Zhongshan Chemical Reagents Co. (Shenyang, China), and the molecular structure of it is displayed in Table 1. Cast iron (0.2–0.9 mm) was obtained from the experimental plant of Institute of Metal Research, Chinese Academy of Sciences (Shenyang, China). Hydrochloric acid and sodium hydroxide were all obtained from Sinopharm Chemical Reagents Co. (Shanghai, China). All chemicals were of analytical grade and were used without any further purification. Distilled water was used throughout this study.

2.2. Experimental procedures

All experiments were carried out in 250 ml beakers, which were placed in a SK250LH ultrasonic cavitation cleaner water bath (Kedao Co. Ltd., China). The temperature was kept constant ($25 \pm 1^\circ\text{C}$) by a cooling coil immersed into the bath. Each exper-

imental run was performed by taking an appropriate amount of stock dye solution followed by the addition of cast iron and dilution with distilled water to 100 ml. Solution pH values were adjusted to the desired level using hydrochloric acid and sodium hydroxide, which were measured by a pH meter (PHS-3C). The reactions were initiated by adding cast iron to the beaker. Samples were taken out from the beaker periodically using a pipette and were immediately analyzed. Each experiment was replicated three times or more.

2.3. Analytical methods

The UV–vis spectra of dye were recorded from 200 to 900 nm using a UV–vis spectrophotometer (Lambda 25, PerkinElmer) with a spectrometric quartz cell (1 cm path length). The maximum absorbance wavelength (λ_{max}) of AR14 could be found at 515 nm from the spectra. Therefore, the concentration of the dye in the reaction mixture at different reaction times was determined by measuring the absorption intensity at $\lambda_{\text{max}} = 515$ nm and from a calibration curve. The degradation efficiency of AR14 was defined as follows:

$$\text{degradation efficiency}(\%) = E = \frac{(C_0 - C)}{C_0} \times 100 \quad (7)$$

where C_0 is the initial concentration of AR14, and C is the concentration of AR14 at reaction time t (min). Drawing the standard curve of AR14 by comparison and analysis of absorbance and the corresponding concentration of AR14.

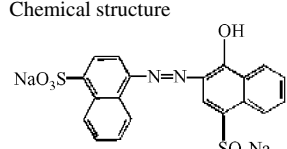
The equation of the standard curve:

$$C_t = 53.616A - 0.1726 \quad (R = 0.9996) \quad (8)$$

The total organic carbon (TOC) of the initial and reacted samples was determined with a TOC analyzer (Multi N/C 3000, Analytikjena, Germany).

AR14 and its degradation products were analyzed by LC–MS systems using a Waters Alliance 2695 autosampler and pumps, a Waters 996 PDA detector and a Waters Micromass ZQ 4000 single quadrupole mass spectrometer (Milford, MA, USA). Chromatography was performed at 30°C on a XBridgeTMC18 column (150 mm \times 3.0 mm, 5 μm , Waters, Ireland) protected by a Security Guard C18 cartridge. CH_3OH , water and acetonitrile (50:50, v/v+ NH_4Ac (0.001 M)) filtered through a 0.2 μm filter were used as mobile phases at flow rates of 0.3 mL min^{-1} . The PDA was set to a wavelength range of 250–260 nm at 1.2 nm resolution. The mass spectrometer was fitted with a Waters Micro-mass 'ESCI' multi-mode ionisation source capable of ionisation in ES and APCI modes in both positive and negative polarities

Table 1
Chemical structure and characteristics of Acid Red 14

Chemical structure	Color index number	λ_{max} (nm)	$\epsilon_{\lambda_{\text{max}}}$ ($\text{L mol}^{-1} \text{ cm}^{-1}$)	Chemical class	M_w (g mol^{-1})
	14720	515	32.658×10^3	Monoazo	502

in a single analysis. The ESCi conditions for negative polarities were as follows: ES capillary voltage 2.80 kV, cone voltage -55.56 V, source temperature 150 °C, desolvation temperature 250 °C, desolvation nitrogen flow 250 L/h, cone nitrogen flow 100 L/h. The mass range was m/z 100–600 scanned over 0.2 s with an interscan delay of 0.1 s, giving a duty cycle of 0.3 s.

3. Results and discussion

3.1. Synergetic effect between cast iron and low frequency ultrasound

All the studies were carried out at the dyes concentration of 50 mg/L. The degradation of AR14 was carried out at three approaches as follows: (1) using the single US, (2) using cast iron and (3) using US–cast iron. As illustrated in Fig. 1, the degradation efficiency of AR14 was enhanced significantly by US. After 10 min reaction in the US–cast iron system, the removal of AR14 was amounted to 90.5%. While the removal efficiency of AR14 by cast iron and US were 49.9% and 4.7%, respectively. The removal of AR14 increased with the prolonged reaction time. The reaction was well followed by the first-order model. The correlation between $\ln C/C_0$ and the reaction time was linear. The kinetic expression can be presented as follows:

$$\ln \frac{C}{C_0} = -k_1 t \quad (9)$$

where C is the AR14 concentration at instant t , C_0 is the initial AR14 concentration, and k_1 is the first-order degradation rate constant and t is the time of reaction.

The first-order rate constants for the degradation of AR14 by cast iron and US–cast iron was $7.50 \times 10^{-2} \text{ min}^{-1}$ ($R^2 = 0.9587$) and $2.58 \times 10^{-1} \text{ min}^{-1}$ ($R^2 = 0.9536$), respectively. The reaction rate was increased by 3.4 times in the presence of ultrasound compared with that of absence of ultrasound. The degradation efficiency of AR14 by US–cast iron was much higher than the sum of the individual effects of cast iron and US, which might due to a synergistic effect.

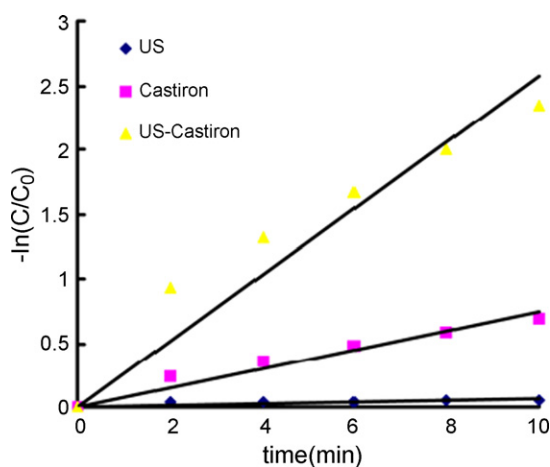
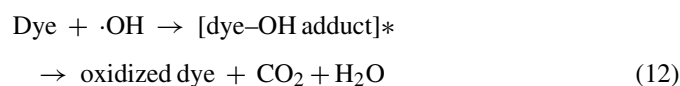
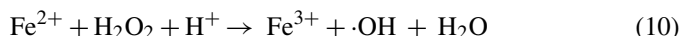


Fig. 1. The first order removal of AR14 by US–cast iron (reaction conditions—pH 6.3; $[\text{Fe}]_0$: 3.0 g; $[\text{dye}]_0$: 50 mg/L; temperature: 25 ± 1 °C; reaction time: 10 min).

In the absence of ultrasound, AR14 molecules transferred from the bulk solution to the vicinity of the cast iron surface, and then were reduced by the reductive species. The degradation products of AR14 and the hydrolysates of iron oxides/hydroxides covered on the cast iron surface, which inhibited the contact between cast iron and the azo dye, and thereby the activity of the cast iron surface was decreased and the further decolorization rate of AR14 was decreased accordingly. The degradation kinetics of azo dyes by cast iron was limited by mass transfer of the substrates to the cast iron surface [22].

In the presence of ultrasonic cavitations, active species such as $\cdot\text{OH}/\cdot\text{OOH}$ could be generated and translated into H_2O_2 during water sonolysis (Eqs. (3–6)). The active species such as $\cdot\text{OH}/\cdot\text{OOH}$ that could also be formed by the inter-reaction of hydrogen peroxide with ferrous and ferric ions from cast iron in aqueous solution according to Eqs. (10) and (11). So, the Fenton's reaction of Fe(II) from cast iron in aqueous solution with sonochemically produced H_2O_2 enhanced degradation of AR14. The main reaction pathway for the degradation of AR14 in solution is the oxidation by $\cdot\text{OH}$ attack (Eq. (12)) [14,23–25].



In addition, during ultrasonic irradiation of liquid–powder slurries, cavitation and the shockwaves it creates can accelerate solid particles to high velocities [26,27]. The interparticle collisions that result are capable of inducing striking changes in surface morphology, composition, and reactivity [27]. Therefore, ultrasonic cavitations led to the cleaning of cast iron, and accordingly more reactant surface area was formed for further surface reactions. The US–cast iron system utilized the actions of the physical effects associated with the continuous ultrasonic cleaning and activation of the cast iron surface. Most of the sediments were separated and transferred into the bulk solution, the AR14 molecules continued to transfer to the vicinity of cast iron surface and the subsequent degradation continued [28].

3.2. The effect of pH on the degradation of AR14

The pH of the solution is an important parameter for cast iron combined with low frequency ultrasonic irradiation, which controls the production rate of hydroxyl radical and the concentration of Fe^{2+} . Fig. 2 illustrates the decolorization of AR14 in US–cast iron system at different pH values. It shows that the residual concentration ($[\text{dye}]_t$) decreased with the decrease of pH. When pH was 2.0, the residual concentration was 3.3 mg/L and the removal rate reached 93.3%, after 10 min treatment. However, when pH rose to 8.0, the residual concentration was 44.31 mg/L and the removal rate dropped to only 11.1%. When effective collision between dye molecule and elemental iron happens, elemental iron, as an electron donor, loses

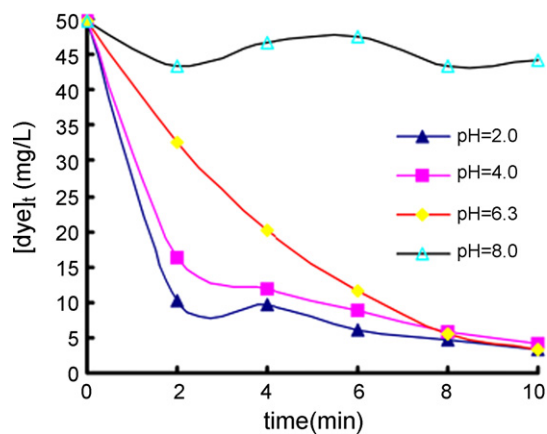


Fig. 2. Effect of pH on the degradation of AR14 (reaction conditions— $[\text{Fe}]_0$: 3.0 g; $[\text{dye}]_0$: 50 mg/L; temperature: $25 \pm 1^\circ\text{C}$; reaction time: 10 min).

electrons, the dye molecule, as an electron acceptor, accepts electrons, combines with H^+ and turns into the transitional product. This product gets electrons from elemental iron and combines with H^+ again, and then it turns into terminal products [29]. As a consequence, pH would enhance overall mass transport [30,31].

3.3. The effect of $[\text{Fe}]_0$ on the degradation of AR14

To elucidate the role of $[\text{Fe}]_0$ on the degradation of AR14 by cast iron combined with low frequency ultrasound, a series of experiments were conducted with different $[\text{Fe}]_0$ from 1.0 g to 5.0 g. Fig. 3 shows the effect of $[\text{Fe}]_0$ on the degradation of AR14 by cast iron combined with low frequency ultrasound. The results indicated that the degradation of AR14 was remarkably dependent on the $[\text{Fe}]_0$ at fixed pH value and $[\text{dye}]_0$. Both degradation efficiency and degradation rate were increased with the increase of $[\text{Fe}]_0$, the degradation efficiency being 64.4%, 92.4% and 96.7% after the 10 min reaction time with $[\text{Fe}]_0$ of 1.0 g, 3.0 g and 5.0 g, respectively. This is because more $\cdot\text{OH}$ radicals are produced with the increase of $[\text{Fe}]_0$ according to Eqs. (1) and (7).

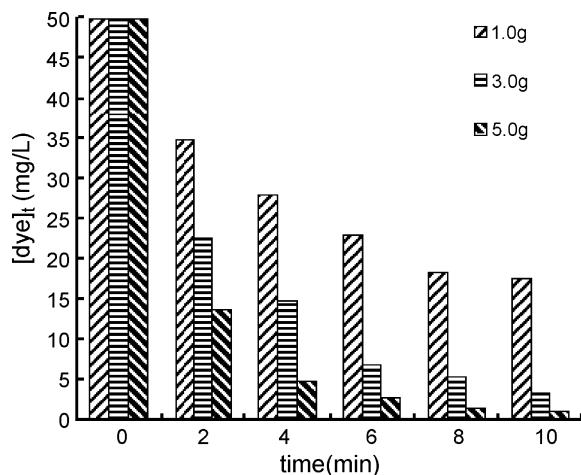


Fig. 3. Effect of $[\text{Fe}]_0$ on the degradation of AR14 (reaction conditions—pH 6.3; $[\text{dye}]_0$: 50 mg/L; temperature: $25 \pm 1^\circ\text{C}$; reaction time: 10 min).

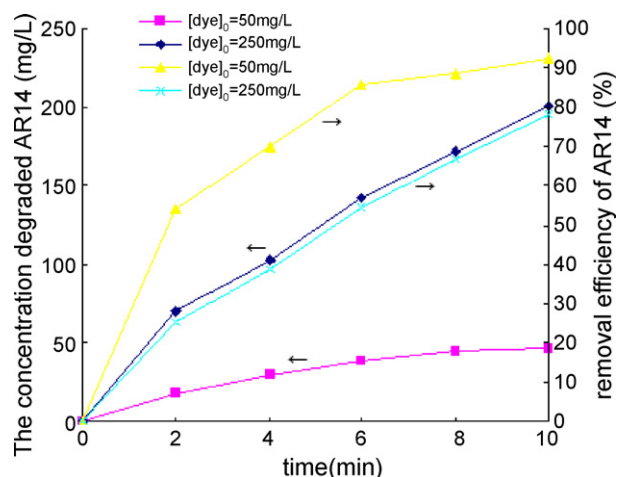


Fig. 4. The effect of $[\text{dye}]_0$ on the degradation of AR14 during US–cast iron system (reaction conditions—pH 6.3; $[\text{Fe}]_0$: 3.0 g; temperature: $25 \pm 1^\circ\text{C}$; reaction time: 10 min).

3.4. The effect of initial dye concentration on the degradation of AR14

Fig. 4 shows the residual concentration of AR14 with the reaction time. When the $[\text{dye}]_0$ is 50 mg/L, the concentration of degraded AR14 and the removal efficiency are 46.38 mg/L and 92.4% after 10 min, respectively. When the $[\text{dye}]_0$ rises to 250 mg/L, the concentration of degraded AR14 and the removal efficiency are 200.38 mg/L and 78.24% after 10 min, respectively. It was observed that lower the $[\text{dye}]_0$ (50 mg/L), shorter is the reaction period needed to degrade AR14 completely. At a higher $[\text{dye}]_0$ of 250 mg/L, the AR14 concentration decreased quickly in the first 2 min and then slowed down as the time goes on. This is due to the fact that with constant $[\text{H}_2\text{O}_2]$ produced by ultrasound and $[\text{Fe}^{2+}]$ from cast iron in aqueous solution, more hydrogen peroxide was consumed in the first 2 min because of a higher $[\text{dye}]_0$. After 2 min, the amount of hydrogen peroxide was smaller and the degradation of AR14 slowed down significantly. In addition, the intermediaries formed may decrease the reaction rate of AR14.

3.5. Mineralization of AR14

Mineralization of AR14 in this process was studied by UV–vis spectrum. We can see, in Table 1, AR14 have azo bond and naphthalene ring. The structures of AR14 were embodied on the UV–vis absorption spectra of their aqueous solutions. AR14 has three absorbance peaks at 218 nm, 317 nm and 515 nm in Fig. 5. AR14 was characterized by one main band in the visible region, with its maximum absorption at 515 nm, and by two bands in the ultraviolet region located at 218 nm and 317 nm. The peaks at 218 nm and 317 nm were ascribed to the absorption of the $\pi-\pi^*$ transition related to the naphthalene rings bonded to the $-\text{N}=\text{N}-$ group in the dye molecule [32,33]. The band in the visible region was attributed to the chromophore-containing azo linkage of the dye molecules in the solution [34].

Extent of mineralization of AR14 can be evaluated by measuring reduction of three absorbance peaks at 218 nm,

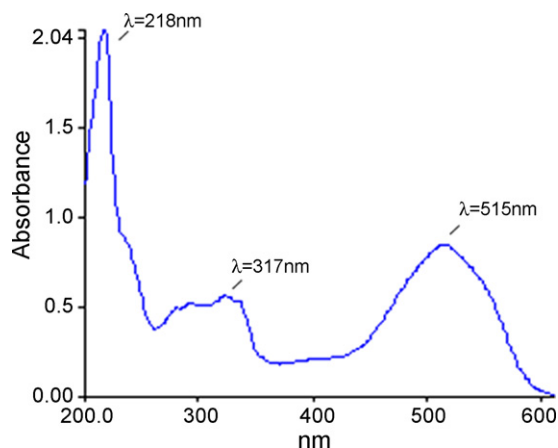


Fig. 5. UV-vis spectra of initial dye solutions: AR14.

317 nm and 515 nm and TOC removal. The reductions of three absorbance peaks were about 37.6%, 46.8% and 97.5%, respectively. The TOC removal of AR14 about 43.2% was observed after 20 min for AR14. A significant mineralization of AR14 was observed in Fig. 6.

3.6. LC-MS study of dyes and their degraded products

As seen in Fig. 7(a), the chromatograms show two major peaks (A and B). It seemed that the dye and dye intermediates could not be well separated in the spectrum, resulting in their overlapping in peak B. Fig. 7(b) shows the mass spectrum of peak A. The signals at 457, 377, 236 and 221/222 m/z in Fig. 7(b) can be ascribed to $[M-2Na+H]^-$, $[M-2Na-SO_3+H]^-$, $[M-2Na-SO_3-C_{10}H_7-OH+4H]^-$ and $[M-2Na-SO_3-C_{10}H_7-OH-NH+4H]^-$, respectively.

Fig. 7(c) represents the HPLC elution profile of AR14 reacted with US-cast iron system for 18 min. It can be seen that the peak A is no more present and instead two new peaks (C and D) with retention time (t_R) at 5.96 min and 8.66 min, respectively was observed. Fig. 7(d) shows the mass spectrum of the product peak C. The signals at 350, 222 and 145 m/z can be ascribed to $[HSO_3C_{10}H_6-C_{10}H_6OH]^-$, $[350-C_{10}H_7]^-$ and

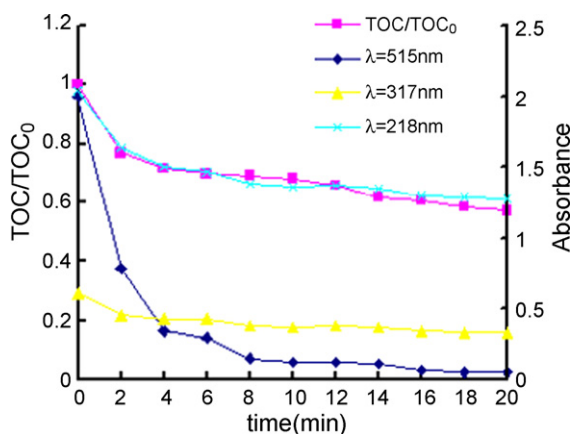


Fig. 6. Mineralization of AR14 (reaction conditions—pH 6.3; $[Fe]_0$: 3.0 g; $[dye]_0$: 50 mg/L; temperature: $25 \pm 1^\circ C$; reaction time: 20 min).

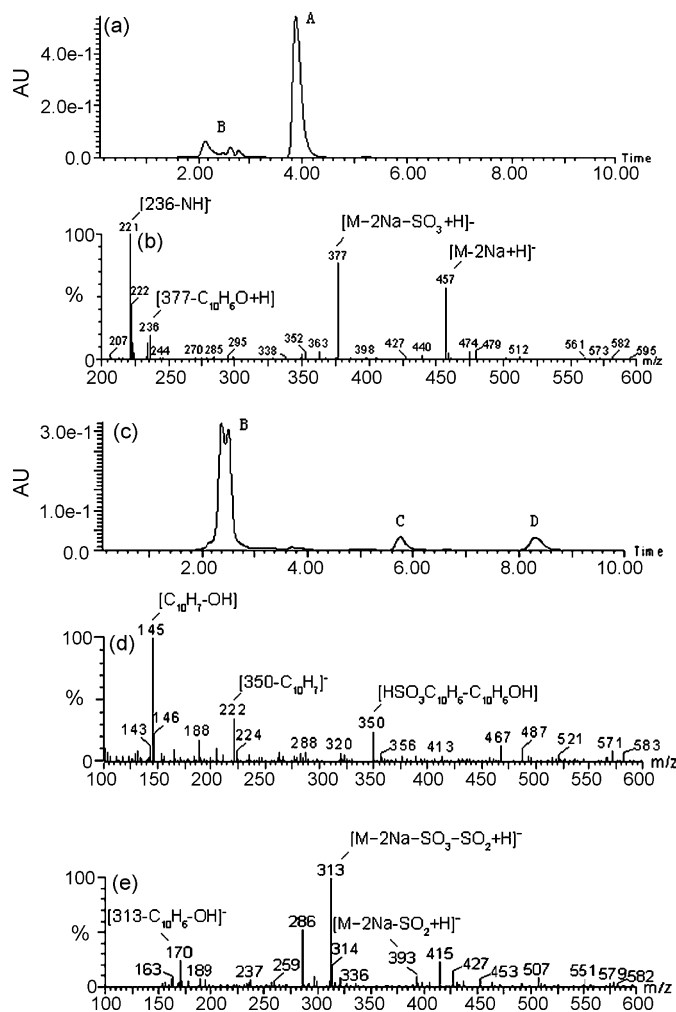


Fig. 7. (a) HPLC elution profile of AR14; (b) mass spectrum for the peak A; (c) HPLC profile of US-cast iron reacted AR14 dye after 18 min reaction time; (d) mass spectrum for the product peak C; (e) mass spectrum for the product peak D. (reaction conditions—pH 6.3; $[Fe]_0$: 3.0 g; $[dye]_0$: 50 mg/L; temperature: $25 \pm 1^\circ C$; reaction time: 20 min).

$[C_{10}H_7-OH]$, respectively. Fig. 7(e) shows the mass spectrum of the product peak D. The signals at 393, 313 and 170 m/z can be ascribed to $[M-2Na-SO_2+H]^-$, $[M-2Na-SO_2-SO_3+H]^-$ and $[M-2Na-SO_2-SO_3-C_{10}H_6OH+H]^-$, respectively. Concluding, azo dye AR14 with a molecular weight of about 457 was decomposed to decolorized metabolite with molecular weights of 350 and 393. Our findings show that hydroxyl radicals react unspecifically by simultaneous hydroxylation and bond scissions of AR14.

4. Conclusions

This study showed the synergistic effect achieved by combining cast iron with low frequency ultrasound radiation for the degradation of C.I. Acid Red 14. The decolorization efficiency decreased with the increasing pH or initial dye concentration, but increased with the increase of the dosage of cast iron. The degradation followed the first-order kinetics model. The first-order rate constant of AR14 degradation by cast iron was $7.50 \times 10^{-2} \text{ min}^{-1}$ while that by US-cast iron

was $2.58 \times 10^{-1} \text{ min}^{-1}$. Accordingly, the degradation rate was improved obviously in the presence of low frequency ultrasound. A significant mineralization of AR14 was observed. The peak (A) almost completely disappeared with US–cast iron system for 18 min. The destruction of the naphthalene rings in azo dyes was slower than that of color which was attributed to the priority of hydroxyl radical attack on the $-\text{N}=\text{N}-$ bonds, and to the formation of numerous oxidation intermediates of organic character during the course of dye degradation.

Acknowledgments

The authors thank the National Key Basic Research and Development Program of China (No. 2004CB418505) and Bureau of Science and Technology of Shenyang Municipality for their financial support to this work.

References

- [1] W. Zhao, Z. Wu, H. Shi, D. Wang, UV photodegradation of azo dye Diacryl Red X-GRL, *J. Photochem. Photobiol. A* 171 (2005) 97–106.
- [2] A.M. Talarposhti, T. Donnelly, G.K. Anderson, Colour removal from a simulated dye wastewater using a two-phase anaerobic packed bed reactor, *Water Res.* 35 (2001) 425–432.
- [3] C.L. Hsueh, Y.H. Huang, C.C. Wang, C.Y. Chen, Degradation of azo dyes using low iron concentration of Fenton and Fenton-like system, *Chemosphere* 58 (2005) 1409–1414.
- [4] B. Lodha, S. Chaudhari, Optimization of Fenton-biological treatment scheme for the treatment of aqueous dye solutions, *J. Hazard. Mater.* 148 (2007) 459–466.
- [5] M. Muruganandham, M. Swaminathan, Decolourisation of Reactive Orange 4 by Fenton and photo-Fenton oxidation technology, *Dyes Pigments* 63 (2004) 315–321.
- [6] H.M. Pinheiro, E. Touraud, O. Thomas, Aromatic amines from azo dye reduction: status review with emphasis on direct UV spectrophotometric detection in textile industry wastewaters, *Dyes Pigments* 61 (2004) 121–139.
- [7] R. Patel, S. Suresh, Decolourization of azo dyes using magnesium–palladium system, *J. Hazard. Mater.* 137 (2006) 1729–1741.
- [8] H. Zhang, L. Duan, Y. Zhang, F. Wu, The use of ultrasound to enhance the decolorization of the CI Acid Orange 7 by zero-valent iron, *Dyes Pigments* 65 (2005) 39–43.
- [9] Y. Ge, L. Yan, K. Qinge, Effect of environment factors on dye decolorization by *P. sordida* ATCC 90872 in a aerated reactor, *Proc. Biochem.* 39 (2004) 1401–1405.
- [10] Y.P. Wang, Treatment of naphthalene derivatives with iron-carbon micro-electrolysis, *Trans. Nonferrous Met. Soc. China* 16 (2006) 1442–1447.
- [11] N. Modirshahla, M.A. Behnajady, S. Kooshaiian, Investigation of the effect of different electrode connections on the removal efficiency of Tartrazine from aqueous solutions by electrocoagulation, *Dyes Pigments* 74 (2007) 249–257.
- [12] Z. Shen, J. Shen, The use of ultrasound to enhance the degradation of the Basic Green by cast iron, *Ultrasonics* 44 (2006) 353–356.
- [13] H. Zhang, M. Jiang, Z.Q. Wang, F. Wu, Decolorisation of C.I. Reactive Black 8 by zero-valent iron powder with/without ultrasonic irradiation, *Color. Technol.* 123 (2007) 203–208.
- [14] J.H. Sun, S.P. Sun, J.Y. Sun, R.X. Sun, L.P. Qiao, H.Q. Guo, M.H. Fan, Degradation of azo dye Acid black 1 using low concentration iron of Fenton process facilitated by ultrasonic irradiation, *Ultrason. Sonochem.* 14 (2007) 761–766.
- [15] E. Psillakis, G. Goula, N. Kalogerakis, D. Mantzavinos, Degradation of polycyclic aromatic hydrocarbons in aqueous solutions by ultrasonic irradiation, *J. Hazard. Mater.* 108 (2004) 95–102.
- [16] A. Khachatryan, R. Sarkissyan, L. Hassratyan, V. Khachatryan, Influence of ultrasound on nanostructural iron formed by electrochemical reduction, *Ultrason. Sonochem.* 11 (2004) 405–408.
- [17] Y. Dai, F. Li, F. Ge, F. Zhu, L. Wu, X. Yang, Mechanism of the enhanced degradation of pentachlorophenol by ultrasound in the presence of elemental iron, *J. Hazard. Mater.* 137 (2006) 1424–1429.
- [18] R.E. Green, Non-contact ultrasonic techniques, *Ultrasonics* 42 (2004) 9–16.
- [19] N.H. Ince, G. Tezcanli-Guyer, Impacts of pH and molecular structure on ultrasonic degradation of azo dyes, *Ultrasonics* 42 (2004) 591–596.
- [20] G. Tezcanli-Guyer, N.H. Ince, I.A. Alaton, Sonochemical destruction of textile dyestuff in wasted dyebaths, *Color. Technol.* 119 (2003) 292–296.
- [21] R. Kidak, N.H. Ince, Ultrasonic destruction of phenol and substituted phenols: A review of current research, *Ultrason. Sonochem.* 13 (2006) 195–199.
- [22] S. Nam, P.G. Tratnyek, Reduction of azo dyes with zero-valent iron, *Water Res.* 34 (2000) 1837–1845.
- [23] N. Kang, D.S. Lee, J. Yoon, Kinetic modeling of fenton oxidation of phenol and monochlorophenols, *Chemosphere* 47 (2002) 915–924.
- [24] S.H. Joo, D. Zhao, Destruction of lindane and atrazine using stabilized iron nanoparticles under aerobic and anaerobic conditions: Effects of catalyst and stabilizer, *Chemosphere* 70 (2008) 418–425.
- [25] S.H. Joo, A.J. Feitz, T.D. Waite, Oxidative degradation of the carbothioate herbicide, molinate, using nanoscale zero-valent iron, *Environ. Sci. Technol.* 38 (2004) 2242–2247.
- [26] Y.X. Li, B.Q. Li, Study on the ultrasonic irradiation of coal water slurry, *Fuel* 79 (2000) 235–241.
- [27] K.S. Suslick, G.J. Price, Applications of ultrasound to materials chemistry, *Annu. Rev. Mater. Sci.* 29 (1999) 295–326.
- [28] H.N. Liu, G.T. Li, J.H. Qu, H.J. Li, Degradation of azo dye Acid Orange 7 in water by Fe_0 /granular activated carbon system in the presence of ultrasound, *J. Hazard. Mater.* 144 (2007) 180–186.
- [29] J. Cao, L. Wei, Q. Huang, L. Wang, S. Han, Reducing degradation of azo dye by zero-valent iron in aqueous solution, *Chemosphere* 38 (1999) 565–571.
- [30] H.M. Hung, M.R. Hoffmann, Kinetics and mechanism of the enhanced reductive degradation of CCl 4 by elemental iron in the presence of ultrasound, *Environ. Sci. Technol.* 32 (1998) 3011–3016.
- [31] H.M. Hung, F.H. Ling, M.R. Hoffmann, Kinetics and mechanism of the enhanced reductive degradation of nitrobenzene by elemental iron in the presence of ultrasound, *Environ. Sci. Technol.* 34 (2000) 1758–1763.
- [32] Y. Xiong, P.J. Strunk, H. Xia, X. Zhu, H.T. Karlsson, Treatment of dye wastewater containing acid orange II using a cell with three-phase three-dimensional electrode, *Water Res.* 35 (2001) 4226–4230.
- [33] F. Wu, N.S. Deng, H.L. Hua, Degradation mechanism of azo dye C. I. reactive red 2 by iron powder reduction and photooxidation in aqueous solutions, *Chemosphere* 41 (2000) 1233–1238.
- [34] A. Wang, J. Qu, J. Ru, H. Liu, J. Ge, Mineralization of an azo dye Acid Red 14 by electro-Fenton's reagent using an activated carbon fiber cathode, *Dyes Pigments* 65 (2005) 227–233.